A Noncoherent Pseudo-Noise Acquisition Scheme for Direct-Sequence Spread-Spectrum Systems Using an Auxiliary Signal

Taweesak Samanchuen and Sawasd Tantaratana

Department of Electrical Engineering, Sirindhorn International Institute of Technology
Thammasat University, Rangsit Campus, Pathumthani , 12121, Thailand
e-mail: taweesak@siit.tu.ac.th, sawasd@siit.tu.ac.th

Abstract

We propose a noncoherent Pseudo-Noise (PN) acquisition scheme for Direct-Sequence Spread-Spectrum (DS/SS) systems using an auxiliary signal, previously used for coherent acquisition. The proposed scheme consists of a phase alignment detector and a voltage controlled clock (VCC) loop, which is for updating the phase of the local PN signal and the direction of update. Performance of the proposed scheme is evaluated by simulation and compared with that of a conventional noncoherent fixed-dwell serial scheme. Results show that the proposed scheme acquires approximately three to four times faster than the conventional scheme. In addition, the variance of the acquisition time of the proposes scheme is 20 to 40 times smaller than that of the conventional scheme.

1. Introduction

One of the major functions of a spread-spectrum system receiver is to generate a local pseudo-noise (PN) signal which is in synchronism with the incoming PN signal. PN synchronization is traditionally achieved in the two steps: coarse synchronization (called acquisition) and fine tuning (called tracking). There has been extensive research on acquisition, see [1-9] for examples. Acquisition schemes may be coherent or noncoherent, depending on whether the receiver knows the carrier phase or not. Generally, the receiver generates a local PN signal and verifies whether or not it aligns with the incoming PN signal to within a specified range (normally within T_c, where T_c is the chip duration) by inspecting the correlation result of the locally generated and the incoming PN signals. If alignment is detected, the tracking circuit is initiated. Otherwise, the local PN signal updates its phase, and the process continues. Acquisition can be classified according to the alignment detection or the phase update strategy (search strategy). Alignment detection may be of fixed-dwell, multiple-dwell, or sequential types. Some phase update strategies are: serial search, Z-search.

Recently, a new acquisition scheme was proposed [10]. An auxiliary signal (instead of the PN signal) was used for correlating with the incoming signal. The auxiliary signal is a linear combination of the PN signal and its shifted versions. By design, the cross-correlation of the auxiliary and the PN signal has a triangle shape with a period equal the period of the PN signal. Such a cross-correlation function enables the receiver to identify the direction of phase update toward the synchronized phase. The proposed scheme was used for coherent acquisition in [10].

In this paper, the idea of using an auxiliary signal is extended to noncoherent acquisition. Section 2 describes the proposed scheme. Section 3 evaluates the probabilities of detection

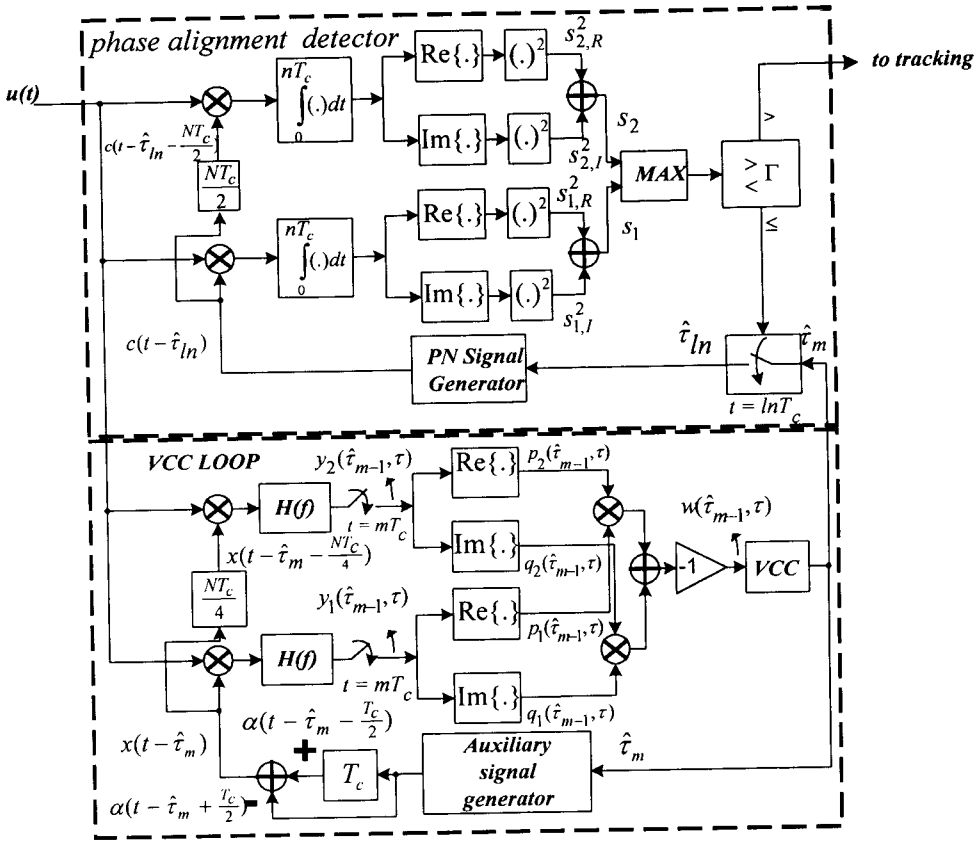

Figure 1: The proposed noncoherent acquisition scheme

and false alarm. Section 4 presents some simulation results. Finally, some concluding remarks are given in Section 5.

2. The Proposed Scheme

The proposed noncoherent acquisition system is depicted in Figure 1. It consists of two parts: voltage controlled clock (VCC) loop and phase alignment detector. The VCC loop uses advanced and delayed versions of an auxiliary signal for correlating with the incoming signal. The auxiliary signal $\alpha(t)$ is designed so that its cross-correlation with the PN signal will indicate the direction for updating the phase of the auxiliary signal. The phase alignment detector decides whether the phase supplied by the VCC loop is within some specified range of the phase of the incoming PN signal. Note that phase alignment detection uses a local PN signal to correlate with the incoming PN signal. In the following subsections we describe the auxiliary signal, the VCC loop, and the alignment detector.

The input signal of the receiver is

$$s(t) = \sqrt{2P}c(t-\tau)\cos(\omega_c t - \theta) + n(t), \quad (1)$$

where $c(t)$ is the PN signal, ω_c and θ are the carrier frequency and phase, P is the average power of the transmitted signal, τ is the phase of the PN signal due to propagation delay, and $n(t)$ is a zero-mean white Gaussian noise with power spectrum density (PSD) of $N_0/2$. For convenience, we use the equivalent baseband signal of $s(t)$, which is

$$u(t) = \sqrt{2P}c(t-\tau)e^{-j\theta} + z(t). \quad (2)$$

The carrier phase θ is assumed to be a uniform random variable, and $z(t)$ is a zero mean white Gaussian process with PSD of $2N_0$. It can be written as

$$z(t) = z_R(t) + jz_I(t), \tag{3}$$

where $z_R(t)$ and $z_I(t)$ are the real part and imaginary part of $z(t)$, respectively.

Let $\hat{\tau}$ be the phase of the local PN signal and auxiliary signal. The phase difference is defined by

$$e_\tau = \hat{\tau} - \tau. \tag{4}$$

The function of an acquisition scheme is to obtain the phase estimate $\hat{\tau}$ such that the error e_τ is within some specified range such as $T_c/2$, where T_c is the chip duration.

2.1 Auxiliary Signal $\alpha(t)$

The auxiliary signal $\alpha(t)$ is defined by

$$\alpha(t) = \sum_{i=-\frac{N-3}{2}}^{\frac{N-3}{2}} \left[\frac{N-1}{2} - |i|\right] c(t - iT_c), \tag{5}$$

where N is the period of the PN sequence $\{c_k\}$, i.e. $c_{k+N} = c_k$, and $c(t)$ is the PN signal given by

$$c(t) = \sum_{k=-\infty}^{\infty} c_k P_{T_c}(t - kT_c), \tag{6}$$

where $c_k = \pm 1$ is the k^{th} chip of the PN sequence. Note that $c(t)$ has a period of NT_c. P_{T_c} is the unit-amplitude rectangular pulse shape in the interval $[0, T_c]$.

An important property of $\alpha(t)$ is its cross-correlation with $c(t)$ which is

$$R_{c\alpha}(\beta) = \frac{1}{NT_c}\int_0^{NT_c} c(t+\beta)\alpha(t)dt$$

$$= \begin{cases} \dfrac{(N-1)(N+3)}{4N} - \dfrac{N+1}{NT_c}|\beta|, & |\beta| \le \dfrac{(N-1)T_c}{2} \\ -\dfrac{(N-1)^2}{4N}, & \dfrac{(N-1)T_c}{2} < \beta < \dfrac{(N+1)T_c}{2} \end{cases} \tag{7}$$

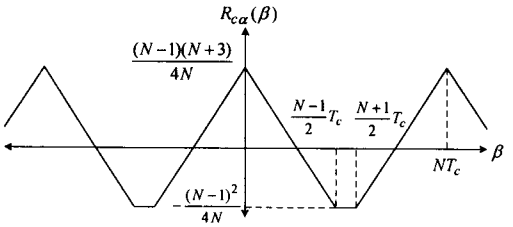

Figure 2: The periodic cross-correlation $R_{c\alpha}(\beta)$

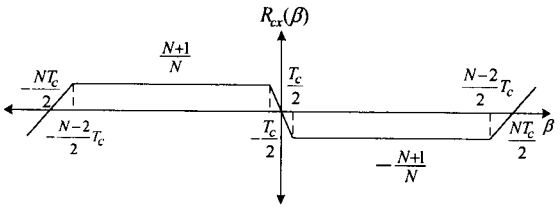

Figure 3: The periodic cross-correlation $R_{cx}(\beta)$

This is plotted in Figure 2. Note that it is periodic with period NT_c, which is the same as the period of $c(t)$.

In the VCC loop, we generate a signal $x(t)$ which is the difference between delayed and advanced versions of $\alpha(t)$. Specifically, we let

$$x(t) = \alpha\left(t - \tfrac{T_c}{2}\right) - \alpha\left(t + \tfrac{T_c}{2}\right). \tag{8}$$

The cross-correlation of $x(t)$ with $c(t)$ is

$$R_{cx}(\beta) = \frac{1}{NT_c}\int_0^{NT_c} c(t+\beta)x(t)dt$$

$$= R_{c\alpha}\left(\beta + \tfrac{T_c}{2}\right) - R_{c\alpha}\left(\beta - \tfrac{T_c}{2}\right), \tag{9}$$

which is shown in Figure 3. It is periodic with period NT_c.

2.2 VCC Loop

The VCC loop is the lower part of Figure 1. The function of this part is to control the phase of the local PN signal by controlling the phase of the auxiliary signal. The received signal $u(t)$ is correlated with $x(t - \hat{\tau}_m)$ and $x(t - \hat{\tau}_m - \frac{NT_c}{4})$. The results of correlation are filtered by $H(f)$ and then sampled at $t = mT_c$, where $m = \{0, 1, 2, \ldots\}$. For noncoherent acquisition, the carrier

phase θ is unknown. Note that noncoherent acquisition is more realistic than coherent acquisition, since θ is normally not available during acquisition. To eliminate the unknown carrier phase, we form two products: one as the product of the real parts of the two signals after filters, and the other is the product of the imaginary parts. The two products are summed and inverted to obtain $w(\hat{\tau}_{m-1},\tau)$.

The VCC computes an estimated $\hat{\tau}_m$ of the phase by updating the previous estimate $\hat{\tau}_{m-1}$ using $w(\hat{\tau}_{m-1},\tau)$. Specifically, the updated estimate is

$$\hat{\tau}_m = \hat{\tau}_{m-1} + K_{VCC}\, w(\hat{\tau}_{m-1},\tau), \qquad (10)$$

where K_{VCC} is a constant, which must be properly chosen. The value K_{VCC} will be determined at the end of this subsection.

Next, we obtain expressions for signals at various points in the VCC loop. The two filters $H(f)$ are chosen to have an impulse response

$$h(t) = \begin{cases} \dfrac{1}{M}, & 0 \le t \le MT_c \\ 0, & \text{otherwise} \end{cases}. \qquad (11)$$

Therefore, it is a moving average filter. The filtered signals can be obtained as

$$y_1(\hat{\tau}_{m-1},\tau) = \frac{\sqrt{2PT_c}}{M} \sum_{k=m-M}^{m-1} \left[v_{k+1}(\hat{\tau}_k,\tau) e^{-j\theta} + \eta_{1,k+1} \right] \qquad (12)$$

and

$$y_2(\hat{\tau}_{m-1},\tau) = \frac{\sqrt{2PT_c}}{M} \sum_{k=m-M}^{m-1} \left[v_{k+1}\left(\hat{\tau}_k + \tfrac{NT_c}{4},\tau\right) e^{-j\theta} + \eta_{2,k+1} \right] \qquad (13)$$

where $v_{k+1}(\cdot,\cdot)$ is a signal component, while $\eta_{1,k+1}$ and $\eta_{2,k+1}$ are noise components given by

$$v_{k+1}(\hat{\tau}_k,\tau) = \frac{1}{T_c} \int_{kT_c}^{(k+1)T_c} c(t-\tau)x(t-\hat{\tau}_k)dt, \qquad (14)$$

$$\eta_{1,k+1} = \frac{1}{\sqrt{2PT_c}} \int_{kT_c}^{(k+1)T_c} z(t)x(t-\hat{\tau}_k)dt, \qquad (15)$$

$$\eta_{2,k+1} = \frac{1}{\sqrt{2PT_c}} \int_{kT_c}^{(k+1)T_c} z(t)x(t-\hat{\tau}_k-\tfrac{NT_c}{4})dt. \qquad (16)$$

The real parts of $y_1(\hat{\tau}_{m-1},\tau)$ and $y_2(\hat{\tau}_{m-1},\tau)$ are

$$p_1(\hat{\tau}_{m-1},\tau) = \frac{\sqrt{2PT_c}}{M}\cos\theta \sum_{k=m-M}^{m-1} v_{k+1}(\hat{\tau}_k,\tau) + \frac{\sqrt{2PT_c}}{M} \sum_{k=m-M}^{m-1} \eta_{R1,k+1}, \qquad (17)$$

$$p_2(\hat{\tau}_{m-1},\tau) = \frac{\sqrt{2PT_c}}{M}\cos\theta \sum_{k=m-M}^{m-1} v_{k+1}\left(\hat{\tau}_k + \tfrac{NT_c}{4},\tau\right) + \frac{\sqrt{2PT_c}}{M} \sum_{k=m-M}^{m-1} \eta_{R2,k+1}, \qquad (18)$$

and the imaginary parts are

$$q_1(\hat{\tau}_{m-1},\tau) = \frac{\sqrt{2PT_c}}{M}\sin\theta \sum_{k=m-M}^{m-1} v_{k+1}(\hat{\tau}_k,\tau) + \frac{\sqrt{2PT_c}}{M} \sum_{k=m-M}^{m-1} \eta_{I1,k+1}, \qquad (19)$$

$$q_2(\hat{\tau}_{m-1},\tau) = \frac{\sqrt{2PT_c}}{M}\sin\theta \sum_{k=m-M}^{m-1} v_{k+1}\left(\hat{\tau}_k + \tfrac{NT_c}{4},\tau\right) + \frac{\sqrt{2PT_c}}{M} \sum_{k=m-M}^{m-1} \eta_{I2,k+1}, \qquad (20)$$

where $\eta_{R1,k+1}$, $\eta_{R2,k+1}$, $\eta_{I1,k+1}$, and $\eta_{I2,k+1}$ are real and imaginary parts of (15) and (16). These are zero-mean Gaussian random variables.

Let us write

$$\hat{\tau}_k - \tau_k = (j_k + \gamma_k)T_c, \qquad (21)$$

$$\hat{\tau}_k + \tfrac{NT_c}{4} - \tau_k = (j'_k + \gamma'_k)T_c. \qquad (22)$$

where j_k and j'_k are integers and γ_k, $\gamma'_k \in (-0.5, 0.5]$. Then we can express the variances of the four noise terms as

$$\sigma^2_{R1,k+1} = \sigma^2_{I1,k+1}$$

$$= \frac{1}{SNR}\left\{(0.5+\gamma_k)(\alpha_{k-1-j_k}-\alpha_{k-j_k})^2 + (0.5-\gamma_k)(\alpha_{k-j_k}-\alpha_{k+1-j_k})^2\right\}, \quad (23)$$

$$\sigma^2_{R2,k+1} = \sigma^2_{I2,k+1} = \frac{1}{SNR}\left\{(0.5+\gamma'_k)(\alpha_{k-1-j'_k}-\alpha_{k-j'_k})^2 + (0.5-\gamma'_k)(\alpha_{k-j'_k}-\alpha_{k+1-j'_k})^2\right\}, \quad (24)$$

where α_k is the k^{th} chip of the auxiliary sequence and SNR is a (per-chip) signal-to-noise ratio given by

$$SNR = \frac{2PT_c}{N_0}. \quad (25)$$

To cancel the effect of θ which is assumed to be a uniform random variable, we form the sum of the products to obtain

$$w(\hat{\tau}_{m-1},\tau) = -[p_1(\hat{\tau}_{m-1},\tau)p_2(\hat{\tau}_{m-1},\tau) + q_1(\hat{\tau}_{m-1},\tau)q_2(\hat{\tau}_{m-1},\tau)], \quad (26)$$

which consists of a signal term and noise terms. Its expected value can be shown to be

$$\overline{w} = E[w(\hat{\tau}_{m-1},\tau)] = -2PT_c^2\left\{\left[R_{c\alpha}\left(e_\tau+\frac{T_c}{2}\right)-R_{c\alpha}\left(e_\tau-\frac{T_c}{2}\right)\right]\left[R_{c\alpha}\left(e_\tau+\frac{(N+2)T_c}{4}\right)-R_{c\alpha}\left(e_\tau+\frac{(N-2)T_c}{4}\right)\right]+\zeta_R+\zeta_I\right\}, \quad (27)$$

where

$$\zeta_R = E\left\{\left(\frac{1}{M}\sum_{k=m-M}^{m-1}\eta_{R1,k+1}\right)\left(\frac{1}{M}\sum_{k=m-M}^{m-1}\eta_{R2,k+1}\right)\right\} = \frac{N+1}{NM(SNR)} \approx \frac{1}{M(SNR)}, \quad (28)$$

and

$$\zeta_I = E\left\{\left(\frac{1}{M}\sum_{k=m-M}^{m-1}\eta_{I1,k+1}\right)\left(\frac{1}{M}\sum_{k=m-M}^{m-1}\eta_{I2,k+1}\right)\right\}$$

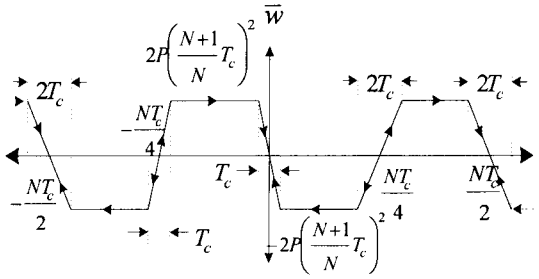

Figure 4: VCC loop discrimination characteristic

$$= \frac{N+1}{NM(SNR)} \approx \frac{1}{M(SNR)}. \quad (29)$$

Since M is a large value, we have $\zeta_R, \zeta_I = 0$, yielding

$$\overline{w} = -2PT_c^2\left[R_{c\alpha}\left(e_\tau+\frac{T_c}{2}\right)-R_{c\alpha}\left(e_\tau-\frac{T_c}{2}\right)\right]\left[R_{c\alpha}\left(e_\tau+\frac{(N+2)T_c}{4}\right)-R_{c\alpha}\left(e_\tau+\frac{(N-2)T_c}{4}\right)\right]. \quad (30)$$

Note that (30) is a product of (9) and its delayed version. It is the delay discriminator characteristic of the VCC loop and plotted in Figure 4, which shows a period of NT_c. We see that there are 2 stable points, at $e_\tau = 0$ and $e_\tau = NT_c/2$. If e_τ is initially in the range of $[-NT_c/4, NT_c/4]$, e_τ will converge to zero. Otherwise e_τ will converge to $NT_c/2$. The pull-in range is $\pm NT_c/4$.

To determine a choice for the constant K_{VCC}, note that each update should not be lager than T_c to avoid jumping over the correct phase, i.e. $|\hat{\tau}_m - \hat{\tau}_{m-1}| \le T_c$. Therefore, from (10) we set the maximum of $nK_{VCC}|\overline{w}|$ to be $\le T_c$, which yields

$$K_{VCC} \le \frac{T_c}{n\max|\overline{w}|} \le \frac{N^2}{2nP(N+1)^2T_c}. \quad (31)$$

If K_{VCC} is small, the update step size is small, which means that the acquisition will be longer. Hence, we use the upper limit in (31) for K_{VCC}.

2.3 Alignment Detection

In Figure 1 the upper part is the alignment detector. The received signal is correlated with two waveforms of the local PN signal. The first has a phase determined by the VCC loop. The phase of the other one is delayed by $NT_c/2$. This is because we need to distinguish the two stable points in Figure 4. The integration length of each correlator is nT_c seconds. The alignment test is performed at $t = lnT_c$, l = 1, 2, ... The magnitude squares of the outputs of the two correlators are compared and the larger one is tested against a threshold. If the threshold is exceeded, the tracking circuit is initiated. Otherwise, the next estimate of $\hat{\tau}$ from the VCC loop is used for the next alignment test. The value n and the threshold Γ need to be designed. This will be discussed in Section 3.

3. Probabilities of Detection and False Alarm

For design and analysis purpose, we formulate the alignment detection as choosing between the following two hypotheses:

$$H_1 : |e_\tau| \le \tfrac{T_c}{2} \text{ or } \tfrac{N-1}{2}T_c \le |e_\tau| \le \tfrac{NT_c}{2} \quad \text{(alignment)}$$
$$H_0 : T_c \le |e_\tau| \le \left(\tfrac{N-2}{2}\right)T_c \quad \text{(no alignment)}. \tag{32}$$

Therefore, H_1 represents phase alignment case, i.e. the phase error is within $\pm T_c/2$ of the two stable points 0 and $NT_c/2$ in Figure 4, while H_0 represents the case that the phase error is at least T_c away from the two stable points. Writing the error as $e_\tau = (j + \gamma)T_c$, where j is an integer and $-0.5 < \gamma \le 0.5$, we may write (32) as

$$\begin{aligned} H_1 :\ & j = 0 && \text{and} && -0.5 < \gamma \le 0.5 \\ & \text{or } j = -1 && \text{and} && \gamma = 0.5 \\ & \text{or } j = \tfrac{N-1}{2} && \text{and} && 0 \le \gamma \le 0.5 \\ & \text{or } j = -\tfrac{N-1}{2} && \text{and} && -0.5 < \gamma \le 0 \end{aligned} \tag{33.1}$$

$$\begin{aligned} H_0 :\ & j \in I = \left\{\tfrac{-N+3}{2}, \tfrac{-N+5}{2}, \ldots, -3, -2, 2, 3, \ldots, \tfrac{N-5}{2}, \tfrac{N-3}{2}\right\} \text{and} -0.5 < \gamma \le 0.5 \\ & \text{or } j = \tfrac{-N+1}{2} \quad \text{and} \quad \gamma = 0.5 \\ & \text{or } j = -1 \quad \text{and} \quad -0.5 < \gamma \le 0 \\ & \text{or } j = 1 \quad \text{and} \quad 0 \le \gamma \le 0.5. \end{aligned} \tag{33.2}$$

Note that the case when $\frac{T_c}{2} < |e_\tau| < T_c$ and $\left(\frac{N}{2} - 1\right)T_c < |e_\tau| < \left(\frac{N-1}{2}\right)T_c$ are not included in either hypothesis, so that there is some distance between H_0 and H_1. Otherwise, the integration length nT_c needs to be excessively large in order that the detector can distinguish between H_0 and H_1, making the acquisition system performance poor.

Detection probability (P_d) and false alarm probability (P_{fa}) of the alignment detector are obtained as follows. Detection probability is the probability that phase alignment is correctly detected, which can occur in two situations. First, given that $|e_\tau| < T_c/2$, we obtain detection when the event $A_1 = \{s_1 > s_2\} \cap \{s_1 > \Gamma\}$ is true, where s_1 and s_2 are the test statistics given in Figure 1. The second case of detection is obtained when A_2 is true given that $\frac{N-1}{2}T_c \le |e_\tau| \le \frac{NT_c}{2}$, where $A_2 = \{s_2 > s_1\} \cap \{s_2 > \Gamma\}$. The probability of detection is the weighted value of these two values. Letting $B_1 = \left\{|e_\tau| \le \frac{T_c}{2}\right.$ and $B_2 = \left\{\frac{N-1}{2}T_c \le |e_\tau| \le \frac{NT_c}{2}\right.$, we have

$$P_d = \frac{\Pr(A_1|B_1)\Pr(B_1) + \Pr(A_2|B_2)\Pr(B_2)}{\Pr(B_1) + \Pr(B_2)}. \tag{34}$$

Since e_τ is equally likely to be anywhere in $[0, NT_c]$, we have $\Pr(B_1) = \Pr(B_2) = 1/N$ and

$$P_d = \frac{\Pr(A_1|B_1) + \Pr(A_2|B_2)}{2}. \tag{35}$$

To compute P_d we note that $s_1 = s_{1,R}^2 + s_{1,I}^2$, $s_2 = s_{2,R}^2 + s_{2,I}^2$ where

$$s_{1,R} = \sqrt{2P}T_c \cos\theta \int_0^{nT_c} c(t - \hat{\tau}_{ln})c(t - \tau)dt + \int_0^{nT_c} c(t - \hat{\tau}_{ln})z_R(t)dt \tag{36}$$

$$s_{1,I} = \sqrt{2P}T_c \sin\theta \int_0^{nT_c} c(t - \hat{\tau}_{ln})c(t - \tau)dt + \int_0^{nT_c} c(t - \hat{\tau}_{ln})z_I(t)dt \tag{37}$$

$$s_{2,R} = \sqrt{2P}T_c \cos\theta \int_0^{nT_c} c\left(t - \hat{\tau}_{ln} - \frac{NT_c}{2}\right)c(t-\tau)dt + \int_0^{nT} c\left(t - \hat{\tau}_{ln} - \frac{NT_c}{2}\right)z_R(t)dt \quad (38)$$

$$s_{2,I} = \sqrt{2P}T_c \sin\theta \int_0^{nT_c} c\left(t - \hat{\tau}_{ln} - \frac{NT_c}{2}\right)c(t-\tau)dt + \int_0^{nT_c} c\left(t - \hat{\tau}_{ln} - \frac{NT_c}{2}\right)z_I(t)dt . \quad (39)$$

Here, $\hat{\tau}_{ln}$ is the phase shift of the local PN signal at time lnT_c. It is shown in Appendix A that

$$P_d = \int_{\Gamma'}^{\infty}\left(1 - Q\left(\sqrt{\frac{SNR}{n}}\lambda\left(n,0,\frac{N+1}{2}\right),\sqrt{x}\right)\right)f_{s_1'}(x|0,0.5)dx \quad (40)$$

where $\Gamma' = \Gamma / nN_0T_c$, $f_{s_1'}(x|j,\gamma)$ is the pdf of $s_1' \triangleq s_1 / nN_0T_c$ when $e_\tau = (j+\gamma)T_c$, given in Appendix A, $Q(\cdot,\cdot)$ is the Marcum Q-function defined as

$$Q(a,b) = \int_b^{\infty} xe^{-(x^2+a^2)/2}I_0(ax)dx \quad (41)$$

and

$$\lambda(n,\gamma,j) = (1-|\gamma|)\sum_{k=0}^{n-1} c_k c_{k-j} + |\gamma|\sum_{k=0}^{n-1} c_k c_{k-j-\mathrm{sgn}(\gamma)} . \quad (42)$$

Here, $I_0(\cdot)$ is the modified Bessel's function of order zero and sgn(t) = 1 if $t \geq 0$ and -1 if $t < 0$.

The false alarm probability is the probability of accepting H_1 given that H_0 is true. When false alarm occurs, the receiver loses some time trying to track the wrong phase. The time spent until the receiver realizes that it cannot track is called penalty time. In this paper a penalty time is assumed to be

$$\text{Penalty time} = K_p nT_c, \quad (43)$$

when K_p is some constant. The region of H_0 is in (32). Therefore, we define P_{fa} as an average probability given by

$$P_{fa} = \frac{1}{(N-4)T_c}\int_{T_c \leq |e_\tau| \leq \left(\frac{N-2}{2}\right)T_c} P_{fa}(e_\tau) \quad (44)$$

where

$$P_{fa}(e_\tau) = \Pr(\text{accept } H_1 \mid T_c \leq |e_\tau| \leq \left(\tfrac{N-2}{2}\right)T_c)$$
$$= 1\text{-}\Pr(\ s_1 < \Gamma \text{ and } s_2 < \Gamma \mid T_c \leq |e_\tau| \leq \left(\tfrac{N-2}{2}\right)T_c).$$

Since $e_\tau = (j+\gamma)T_c$, we write $P_{fa}(e_\tau)$ as

$$P_{fa}(j,\gamma) = 1 - \left[\int_0^{\Gamma'} f_{s_1'}(x|j,\gamma)dx\right]\left[\int_0^{\Gamma'} f_{s_2'}(y|j,\gamma)dy\right]. \quad (45)$$

Substitute (45) into (44) and rewrite the result using Q-function, (44) becomes

$$\begin{aligned} P_{fa} = 1 - \frac{1}{N-4}\Bigg\{ & \sum_{j\in I}\int_{-0.5}^{0.5}\left[1 - Q\left(\sqrt{\frac{SNR}{n}}\lambda(n,\gamma,j),\sqrt{\Gamma'}\right)\right] \\ & \cdot\left[1 - Q\left(\sqrt{\frac{SNR}{n}}\lambda\left(n,\gamma-\frac{\mathrm{sgn}(\gamma)}{2}, j+\frac{N+\mathrm{sgn}(\gamma)}{2}\right),\sqrt{\Gamma'}\right)\right]d\gamma \\ & + \int_{-0.5}^{0}\left[1 - Q\left(\sqrt{\frac{SNR}{n}}\lambda(n,\gamma,-1),\sqrt{\Gamma'}\right)\right] \\ & \cdot\left[1 - Q\left(\sqrt{\frac{SNR}{n}}\lambda(n,\gamma+0.5,\tfrac{N-1}{2}),\sqrt{\Gamma'}\right)\right]d\gamma \\ & + \int_{0}^{0.5}\left[1 - Q\left(\sqrt{\frac{SNR}{n}}\lambda(n,\gamma,1),\sqrt{\Gamma'}\right)\right] \\ & \cdot\left[1 - Q\left(\sqrt{\frac{SNR}{n}}\lambda(n,\gamma-0.5,\tfrac{N+3}{2}),\sqrt{\Gamma'}\right)\right]d\gamma \Bigg\} \end{aligned} \quad (46)$$

where I is given in (33.2).

Given the desired values of P_d and P_{fa}, the value of n and Γ can be computed numerically from (40) and (46).

4. Simulation Results

Performance of the proposed scheme is evaluated by simulation, using the equivalent baseband model, according to Figure 1. The initial phase of the received signal τ for each simulation was set to a multiple of T_c. The initial local PN phase was set so that the phase difference is equally distributed over all the possible range.

In the simulations, we obtained both the mean acquisition time and the variance of the acquisition time of the proposed scheme.

SNR (dB)	P_d	P_{fa}	Correlation time		K_p	Results for Conventional scheme	
			Proposed scheme(n)	Conventional Scheme(n')		Mean acq. time ($/T_c$)	Variance of acq. time ($/1{,}000T_c$)^2
-5	0.9	0.1	179	130	20	90,869	11,825
-5	0.9	0.1	179	130	50	147,586	30,130
-5	0.95	0.05	240	180	20	85,744	11,271
0	0.95	0.05	70	64	20	34,938	1,127

Table 1: Parameter values used in the simulation and simulation results for conventional noncoherent serial acquisition scheme

The PN signal in the simulations is generated from the m-sequence with polynomial $1+x^4+x^9$, i.e. $N = 511$. The simulations were carried out in 4 cases, with the parameter values shown in Table 1. In each case, the same SNR, P_d, P_{fa} and K_p were used for both the proposed scheme and the conventional scheme. The correlation lengths for test alignment of the two schemes are indicated in Table 1. In each case of simulations the parameter M of the filter $H(f)$ in the proposed scheme is varied from 500 to 12,000.

Results of the mean acquisition time and the variance of the acquisition time are given in Table 1 for the conventional scheme, while they are plotted in Figures 5 and 6 for the proposed scheme. Figures 5 and 6 show that the mean and variance are reasonably stable for a wide range of M. When M is too small, the acquisition time of the proposed scheme increases. Recall that MT_c is the length of the filter in the VCC loop. Therefore, a small M will make the filter less effective in filtering out noise. On the other hand, if M too large, the VCC loop will take unnecessarily long time to perform the filtering, leading to inefficiency.

To compare the two schemes, we define two ratios R_1 and R_2 as

$$R_1 = \frac{\overline{T}_{serial}}{\overline{T}_{cl}}, \qquad (47)$$

where $\overline{T}_{serial}$ and $\overline{T}_{cl}$ are the mean acquisition times of the conventional scheme and the proposed closed loop scheme, respectively, and

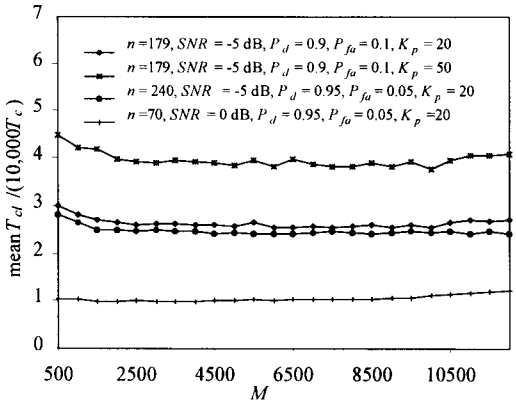

Figure 5: Mean acquisition time of the proposed scheme

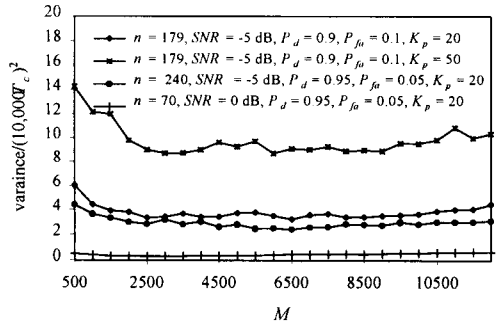

Figure 6: Variance of the acquisition time of the proposed scheme

$$R_2 = \frac{\sigma^2_{serial}}{\sigma^2_{cl}}, \qquad (48)$$

where σ^2_{serial} and σ^2_{cl} are the variances of the acquisition time of the conventional scheme and the proposed scheme, respectively. Results for R_1 and R_2 are plotted in Figures 7 and 8, respectively. From Figure 7, we find that the proposed scheme acquires the correct phase three to four times faster than the conventional scheme. In Figure 8 we see that the variance of the acquisition time of the proposed scheme is smaller than that of the conventional scheme by 20 to 40 times.

From the simulation results, we see that the performance of the proposed scheme is better than that of the conventional scheme. However, the proposed scheme uses more hardware than the conventional scheme, which is a trade-off.

5. Conclusion

A closed-loop noncoherent PN acquisition scheme for DS/SS systems was proposed. The system consists of two subsystems: the VCC loop and the phase alignment detector. An auxiliary signal is used in the VCC loop so that the loop adjusts the phase difference between the auxiliary signal and the incoming PN signal towards one of the two stable points. The phase alignment detector periodically checks to see if the phase difference is sufficiently close to one of the two stable points. If it is, the tracking circuit is initiated. Otherwise, the VCC loop keeps on adjusting itself.

The performance of the proposed scheme was evaluated by simulation. It was found that the proposed scheme acquires the phase much faster than the conventional noncoherent serial scheme by 3-4 folds, with a reduction in the variance of the acquisition time by 20 to 40 times.

Acknowledgement:

This work was supported in parts through a Telecommunications Consortium scholarship from the National Science and Technology Development Agency (NSTDA), Bangkok, Thailand.

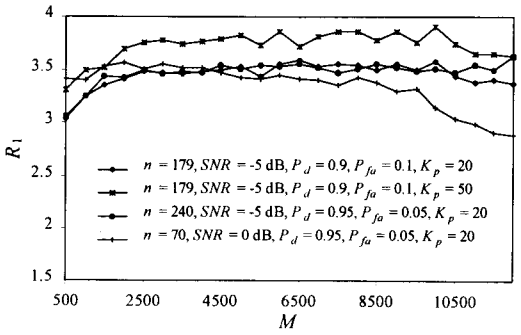

Figure 7: Ratio of the mean acquisition time of the conventional noncoherent serial scheme to that of the proposed scheme

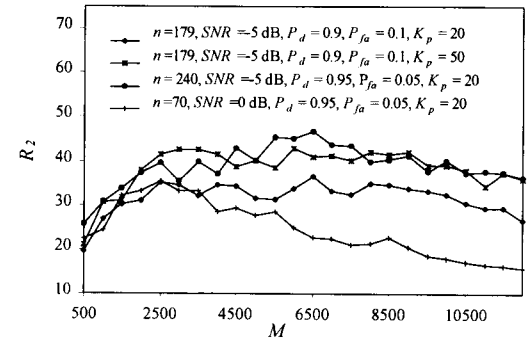

Figure 8: Ratio of the variance of the acquisition time of the conventional noncoherent serial scheme to that of the proposed scheme

List of Symbols

Symbol	Definition
A_1	the event that $s_1 > s_2$ and $s_1 > \Gamma$
A_2	the event that $s_2 > s_1$ and $s_2 > \Gamma$
$\alpha(t)$	auxiliary signal
B_1	the event $\lvert e_\tau \rvert \le \frac{T_c}{2}$
B_2	the event $\frac{N-1}{2} T_c \le \lvert e_\tau \rvert \le \frac{NT_c}{2}$
$c(t)$	pseudo-noise (PN) signal
$E(\cdot)$	expectation operator
e_τ	phase difference between τ and $\hat{\tau}$
η	noise

$f_x(t)$ probability density function of x
Γ threshold level in the phase alignment detector
γ fractional part of the phase difference
$H(f)$ frequency response of the filter
H_0, H_1 hypotheses in phase alignment detection
$h(t)$ impulse response function of the filter
$I_0(\cdot)$ modified Bessel function of 1st kind and order zero
j integer part of the phase difference
K_p constant of penalty time
K_{VCC} gain of voltage controlled clock
M filter length
N the period of an m-sequence
N_0 level of power spectrum density of noise
nT_c integration length
$n'T_c$ integration length of the conventional scheme
$n(t)$ a zero mean AWGN
ω_c carrier frequency
P power of the received signal
P_d detection probability
P_{fa} false alarm probability
p real-part signal
q imaginary-part signal
$R(\beta)$ correlation function
R_1 ratio of the mean acquisition times
R_2 ratio of the variances of acquisition time
SNR signal-to-noise ratio
$s(t)$ received signal
s_1 signal on branch 1 of the phase alignment detector
s_2 signal on branch 2 of the phase alignment detector
σ^2 noise variance
σ_{cl}^2 variance of the acquisition time of the noncoherent proposed scheme
σ_{serial}^2 variance of the acquisition time of the noncoherent serial search scheme
θ carrier phase
T_c chip duration
$\overline{T}_{cl}$ mean acquisition time of the proposed noncoherent scheme
$\overline{T}_{serial}$ mean acquisition time of the noncoherent serial search scheme
τ phase shift of the received PN signal
$u(t)$ equivalent baseband of the non-coherent received signal
$v(t)$ signal component of y
w the processed signal used to control the voltage controlled clock
$x(t)$ the difference between the delayed and advanced versions of $\alpha(t)$
$z(t)$ complex envelope of $n(t)$
ζ expected value of the noise

Appendix A Derivation of the Detection Probability

The second terms of $s_{1,R}$ and $s_{1,I}$ in (36) and (37) are the noise terms which can be shown to be independent and identically distributed (iid) random variables. Similarly, the noise components of $s_{2,R}$ and $s_{2,I}$ are iid. These four noise terms are Gaussian random variables with zero mean and the same variance of

$$\sigma_{1,R}^2 = \sigma_{1,I}^2 = \sigma_{2,R}^2 = \sigma_{2,I}^2 = nN_0T_c . \qquad (A.1)$$

It follows that s_1 and s_2 are chi-square random variables with 2 degrees of freedom [11]

$$f_{s_1}(x) = \begin{cases} \frac{1}{2nN_0T_c} e^{-\frac{x+g^2(\hat{\tau},\tau)}{2nN_0T_c}} I_0\left(\frac{g(\hat{\tau},\tau)\sqrt{x}}{nN_0T_c}\right), & x \geq 0 \\ 0, & x < 0 \end{cases} \qquad (A.2)$$

and

$$f_{s_2}(y)=\begin{cases}\frac{1}{2nN_0T_c}e^{-\frac{y+g^2\left(\hat{\tau}+\frac{NT_c}{2},\tau\right)}{2nN_0T_c}} & \\ \cdot I_0\left(\frac{g\left(\hat{\tau}+\frac{NT_c}{2},\tau\right)\sqrt{y}}{nN_0T_c}\right), & y\geq 0 \\ 0, & y<0\end{cases} \quad (A.3)$$

where

$$g(\hat{\tau},\tau)=\sqrt{2P}\int_0^{nT_c}c(t-\hat{\tau})c(t-\tau)dt\,. \quad (A.4)$$

Note that here we write $\hat{\tau}$ for $\hat{\tau}_{lm}$.

The correlation coefficient ρ of $s_{1,R}$ and $s_{2,R}$ is

$$\rho=\frac{E\{s_{1,R}s_{2,R}\}}{\sigma_{1,R}\sigma_{2,R}}=\frac{1}{nT_c}\int_0^{nT_c}c(t-\tau)c(t-\tau-\frac{NT_c}{2})dt \approx 0 \quad (A.5)$$

Therefore, $s_{1,R}$ and $s_{2,R}$ are approximately uncorrelated. Since they are jointly Gaussian, they are also statistically independent. Similarly, $s_{1,I}$ and $s_{2,I}$ are also independent. Therefore, s_1 is statistically independent of s_2.

The quantity $g(\hat{\tau},\tau)$ can be written in terms of j and γ as

$$g(\hat{\tau},\tau)=\sqrt{2P}T_c\lambda(n,\gamma,j) \quad (A.6)$$

where $\lambda(n,\gamma,j)$ is given by (42). Letting

$$s_1'=\frac{s_1}{nN_0T_c},\quad s_2'=\frac{s_2}{nN_0T_c}, \quad (A.7)$$

the pdf's in (A.2) and (A.3) can be put in different forms as

$$f_{s_1'}(x|j,\gamma)=\begin{cases}\frac{1}{2}e^{-\left[\frac{x}{2}+\frac{SNR}{2n}\lambda^2(n,\gamma,j)\right]} & \\ \cdot I_0\left(\sqrt{\frac{SNR}{n}}\lambda(n,\gamma,j)\sqrt{x}\right) & x\geq 0 \\ 0 & x<0\end{cases} \quad (A.8)$$

where SNR is given by (25) and

$$f_{s_2'}(y|j,\gamma)=\begin{cases}\frac{1}{2}e^{-\left[\frac{y}{2}+\frac{SNR}{2n}\lambda^2\left(n,\gamma-\frac{\mathrm{sgn}(\gamma)}{2},j+\frac{N+\mathrm{sgn}(\gamma)}{2}\right)\right]} & \\ \cdot I_0\left(\sqrt{\frac{SNR}{n}}\lambda\left(n,\gamma-\frac{\mathrm{sgn}(\gamma)}{2},\right.\right. & \\ \left.\left.j+\frac{N+\mathrm{sgn}(\gamma)}{2}\right)\sqrt{y}\right) & y\geq 0 \\ 0 & y<0\end{cases} \quad (A.9)$$

Examples of the pdf (A.8) are plotted in Figure 9 for some parameter values.

Since s_1 and s_2 are independent, the joint pdf of s_1' and s_2' can be written as

$$f_{s_1',s_2'}(x,y|j,\gamma)=f_{s_1'}(x|j,\gamma)f_{s_2'}(y|j,\gamma). \quad (A.10)$$

The detection probability is smallest (worst case) when the phase difference e_τ is half a chip off from either one of the locking points $e_\tau=0$ and $e_\tau=NT_c/2$, i.e., when $e_\tau=0.5T_c$ ($j=0$ and $\gamma=0.5$) or $e_\tau=-\frac{N-1}{2}T_c$ $\left(j=-\frac{N-1}{2},\gamma=0\right)$, yielding.

$$P_d=\frac{1}{2}\left\{\int_{\Gamma'}^{\infty}\int_0^x f_{s_1',s_2'}(x,y|0,0.5)dydx + \int_{\Gamma'}^{\infty}\int_0^y f_{s_1',s_2'}\left(x,y|-\tfrac{N-1}{2},0\right)dxdy\right\}, \quad (A.11)$$

where $\Gamma'=\Gamma/nN_0T_c$. Substitute (A.8) and (A.9) into (A.11), the two terms are equal, so we have

$$P_d=\int_{\Gamma'}^{\infty}\int_0^x f_{s_1',s_2'}(x,y|0,0.5)dydx\,. \quad (A.12)$$

Substituting $f_{s_1',s_2'}(x,y|0,0.5)$ and evaluating yields (40).

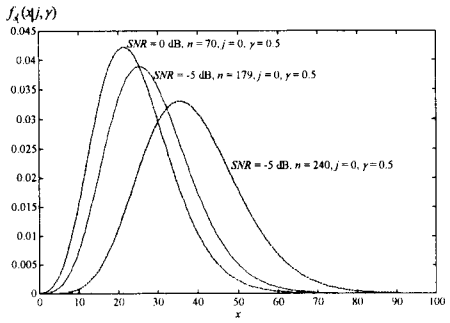

Figure 9: The probability density function of $f_{S_1}(x|j,\gamma)$ at various conditions

References

[1] Simon, M. K., Omura, J.K., Scholtz, R. A. and Levitt, B. K., (1985), *Spread spectrum Communications Handbook*, McGraw-Hill.

[2] Dicarlo, D. M. and Weber, C. L. (1980), Statistical Performance of Single Dwell Serial Synchronization Systems, *IEEE Transactions on Communications*, Vol. COM-28, No. 8.

[3] Glisic, S. G. and (1988), Automatic Decision Threshold Level Control (ADTLC) in Direct-Sequence Spread-Spectrum Systems Based on Matched Filtering, *IEEE Transactions on Communications*, Vol. 36, No. 4.

[4] Jovanovic, V. M. and (1988), Analysis of Strategies for Serial-Search Spread-Spectrum Code Acquisition-Direct Approach, *IEEE Transactions on Communications*, Vol. 36, No. 11.

[5] Lee, Y. H. and Tantaratana, S., (1992), Sequential Acquisition of PN Sequences for DS/SS Communication, *IEEE Journal on Selected Areas in Communications*, Vol. 10, No. 4.

[6] Barghouthi, R. T. and Stuber, G. L. (1994), Rapid Sequence Acquisition for DS/CDMA Systems Employing Kasami Sequences, *IEEE Transactions on Communications*, Vol. 42, No. 2/3/4.

[7] Tantaratana, S., Lam, A. W. and Vincent, P. J. (1995), Noncoherent Sequential Acquisition of PN Sequences for DS/SS Communications with/without Channel Fading, *IEEE Transactions on Communications*, Vol. 43, No. 2/3/4.

[8] Pan, S. M., Grant, H. A. Dodds, D. E. and Kumar, A. (1995), An Offset-Z Search Strategy for Spread Spectrum Systems, *IEEE Transactions on Communications*, Vol. 43, No. 12.

[9] Agee, B. G., Kleinman, R. J. and Reed, J. H. No(1996), Soft Synchronization of Direct Sequence Spread-Spectrum Signal, *IEEE Transaction on Communications*, Vol. 44, No. 11.

[10] Salih, M. and Tantaratana, S. (1996), A Closed-Loop Coherent Acquisition Scheme for PN Sequence Using an Auxiliary Sequence, *IEEE Journal on Selected Area in Communications*, Vol. 14, No. 8.

[11] Simon, M. V., Hinedi, S. M. and Lindsey, W. C. (1995), Signal Design and Detection, *Digital Communication Techniques*, Prentice Hall.